Journal of Applied Physics

Entanglement density and particle dynamics in rigid interfacial layers of polymer nanocomposites

Cite as: J. Appl. Phys. **130**, 064701 (2021); https://doi.org/10.1063/5.0060139
Submitted: 15 June 2021 . Accepted: 26 July 2021 . Published Online: 10 August 2021

Di Wu, Yi Feng, Ruhao Li, Rahmi Ozisik, and Pinar Akcora

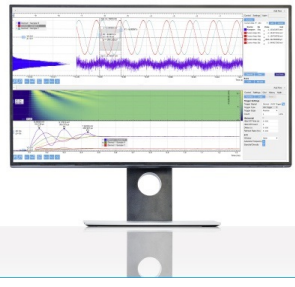

Journal of Applied Physics ARTICLE scitation.org/journal/jap

Entanglement density and particle dynamics in rigid interfacial layers of polymer nanocomposites

Cite as: J. Appl. Phys. 130, 064701 (2021); doi: 10.1063/5.0060139
Submitted: 15 June 2021 · Accepted: 26 July 2021 ·
Published Online: 10 August 2021

Di Wu,[1] Yi Feng,[1] Ruhao Li,[1] Rahmi Ozisik,[2] and Pinar Akcora[1,a)]

AFFILIATIONS

[1]Department of Chemical Engineering & Materials Science, Stevens Institute of Technology, Hoboken, New Jersey 07030, USA
[2]Department of Materials Science and Engineering, Rensselaer Polytechnic Institute, Troy, New York 12180, USA

[a)]**Author to whom correspondence should be addressed:** pakcora@stevens.edu

ABSTRACT

Intermixing between chemically different polymers around nanoparticles creates chemically heterogeneous layers, exhibiting unusual dynamic anomalies due to dynamic confinement and coupling phenomena in polymer nanocomposites. Interfacial mixing of chains is possible when adsorbed chains are mobile above their glass-transition temperature, leading to enhanced entanglement density at the interphase. Linear rheology data of polymer nanocomposites with chemically heterogeneous interphases around nanoparticles were analyzed over a wide frequency range to investigate the role of chain rigidity on matrix chain relaxations and particle diffusion. Our findings show that nanoparticles adsorbed with less rigid polymer move in a sub-diffusive mode. Nanoparticles adsorbed by flexible polymers can slow down the matrix polymer dynamics and particle diffusion, and this interphase effect enhances the viscoelastic properties of the whole polymer nanocomposite.

I. INTRODUCTION

Particle–polymer interactions and the interfacial layers where particles and polymer interact at varying strength and length scale control thermo-mechanical properties of polymer nanocomposites.[1–6] Dynamics and structures of interfacial layers are important for understanding the reinforcement and viscoelastic properties of composites. Viscosity, fragility, and glass-transition temperature of interfacial layers are controlled by interactions between particles and chains.[7–17]

We recently showed that linear, amorphous, and weakly interacting polymer blends in the presence of nanoparticles reversibly stiffen at high temperatures due to differences in chain relaxations between adsorbed and matrix polymers occurring at dynamically asymmetric interphases around nanoparticles.[3,16] The chemical architecture of chains on particles, either they are adsorbed or grafted, influences the stiffening behavior of composites.[12] For example, the poly(methyl methacrylate) (PMMA)-adsorbed and PMMA-grafted particles in poly(ethylene oxide) (PEO) matrices exhibited different temperature dependent viscoelastic moduli.[12] PEO composites of adsorbed particles reinforced and presented thermal stiffening behavior, whereas PEO composites of grafted particles thermally softened and exhibited more elastic behavior at high temperature compared to the low temperature response.[12] The linear and non-linear rheology results of adsorbed and grafted particle systems in the same host matrix and particle loadings reveal the role of high-T_g polymer conformations on interfacial dynamics.

To understand the effect of T_g differences (ΔT_g) between adsorbed and matrix polymers on the observed stiffening behavior, we studied another system of poly(methyl acrylate) (PMA) composite with poly(vinyl acetate) (PVAc) adsorbed particles.[1] PMA–PVAc is a miscible polymer blend with a small ΔT_g of 25 °C. We found that in this attractive composite, reinforcement was enhanced with the use of 40 kDa PMA chains as compared to 140 kDa PMA; however, thermal stiffening was not observed.[1] In the PMMA–PMA blend system, with a ΔT_g of 90 °C, the adsorbed particles in the short matrix formed an elastic network and the composite was reinforced above the T_g of PMMA.[1] The interphase mixing of grafted chains with the matrix polymers was studied in another work by measuring the particle relaxations in x-ray photon correlation spectroscopy (XPCS) experiments.[18] It was reported

that particles in aggregated systems experience a dynamically heterogeneous environment displaying hyper-diffusive relaxation, whereas with less penetration of long matrix chains, particles move in the diffusive mode.[18] These results suggest that particle motion is dictated by the strong interactions of chains grafted at low density with the host polymer.

Moreover, lowering the rigidity of adsorbed polymers enhances the entanglement density and elastic moduli of composites.[2] Rigidity of a polymer is described by its characteristic ratio, C_∞. Temperature sweep tests showed that composite of poly(2-vinyl pyridine) (P2VP) ($C_\infty = 10$) coated particles softened; composite of PMMA coated particles (with $C_\infty = 7$) had an upturn in the elastic modulus; and composite of PC (with $C_\infty = 2.4$) behaved as a gel with the highest elastic modulus measured at 185 °C (above $T_{g,PMMA}$). These results verified that interphase controlled viscoelastic properties in polymer nanocomposites can be regulated with the rigidity of adsorbed chains. It was proposed that when adsorbed chains are less rigid (i.e., flexible like PMMA), the matrix can easily entangle with adsorbed chains and slow down the interfacial layer dynamics.[2] This work aims to understand the slowing down of the matrix chains through the chain entanglements and particle diffusion by analysis of rheology data.

II. EXPERIMENTAL SECTION

A. Sample preparation

Iron oxide (Fe_3O_4) nanoparticles (15 ± 3 nm in diameter) purchased from Rosecreek Technologies Inc. were surface modified with APTES {[(3-aminopropyl)triethoxysilane], 99%, Sigma-Aldrich} following the procedure reported in our previous work.[7] PMMA (35 kDa, PDI = 1.1) was synthesized via atom transfer radical polymerization (ATRP). PMMA and PVAc (50 kDa, Wacker Chemie} were both dissolved in acetonitrile, and P2VP (40 kDa, Polysciences, Inc.) was dissolved in dichlorobenzene. The concentration of the polymer was 15 mg/ml in all solutions. 5 mg/ml–NH_2 modified Fe_3O_4 (NH_2–Fe_3O_4) nanoparticle solution was added to the polymer solution and then sonicated for 10 min followed by 30 min rigorous stirring. Polymer adsorbed NH_2–Fe_3O_4 nanoparticles were collected by centrifuge and washed with the corresponding solvent several times to remove all free polymers. They were then dried under vacuum at room temperature. Dried nanoparticles were mixed with poly(methyl acrylate) (PMA 40 kDa, Sigma-Aldrich, $\rho = 1.22$ g/cm^3, $T_g = 10$ °C) in acetonitrile. Solutions were cast to form composite films, which were annealed at 130 °C for three days. Particle loading in all composites is around 30 wt. % (10 vol. %). This percentage is for the core particles only, and it does not include the adsorbed chains. PMA and adsorbed polymers (PMMA, P2VP, and PVAc) are all miscible, and binary interaction values of polymer pairs are provided in the supplementary material.

B. Thermal analysis

The amount of adsorbed polymer was determined by a TA Q50 thermogravimetric analyzer (TGA). Samples were pre-heated at 150 °C for 20 min and then heated to 550 °C at a 5 °C/min heating rate. TGA curves for bare and polymer adsorbed NH_2–Fe_3O_4 nanoparticles are shown in Fig. S1 in the supplementary material.

C. Rheology experiments

Linear viscoelastic (LVE) data of polymer nanocomposite melts was measured in ARES-G2 strain-controlled rheometer using 8-mm parallel plates. Time–temperature superposition (TTS) curves were obtained for a wide frequency range measured at 35, 55, 85, and 140 °C. The reference temperature of 35 °C was above the glass-transition temperature of PMA ($T_{g,PMA}$: 10 °C).

D. Small-angle x-ray scattering analysis

Small-angle x-ray scattering (SAXS) experiments were performed at the NSLS-II 12-ID beamline at the Brookhaven National Laboratory. The sample to detector distance was 8.3 m, and data were collected at the 0.005–0.15 Å^{-1} q range. NIKA software package[19] was employed to process 2D SAXS data. 1D SAXS plots were generated by integrating the 2D SAXS data after background correction. The SAXS data were fitted by the Unified Model[20] as described in the supplementary material.

E. Transmission electron microscope

Polymer adsorbed NH_2–Fe_3O_4 composites were cryotomed and then imaged in a JEOL USA JEM-2100Plus transmission electron microscope operated at 200 kV and equipped with a cold-field emission gun.

F. TTS data fitting and analysis of particle dynamics

The linear viscoelastic response of polymer nanocomposites includes the hydrodynamic contribution from the nanoparticles. Thus, the effective diffusion of nanoparticles is related to the linear rheological response. A recent work by You and Yu evaluated the multistage diffusion of nanoparticles in polymer melts via chain entanglement network and particle caging.[21] At time scales longer than the terminal relaxation time of the polymer matrix, the rheological data were analyzed by a model considering hydrodynamic contributions, confined diffusion within chain entanglements, and confined diffusion in nanoparticle cages.[21] Equation (1) shows the model equation describing the short and intermediate time scale relaxations. Long time relaxation for particle caging is not added to the model because the particle network relaxation is barely reached in the experimental time scale. τ_t is the terminal relaxation, G_N is the rubber plateau modulus of composites, and n is the confining diffusion exponent. G_N, τ_t, and n are the fitting parameters to this model equation. G^*_{PNC} is the complex modulus of the polymer nanocomposite, a_r is the strain rate amplitude factor, a_s is the stress rate amplitude factor, $G^*_m(\omega)$ is the complex modulus contribution from the matrix, and Γ is the gamma function. The effective particle volume fraction, $\phi_{p,eff}$, is 0.1,

$$G^*_{PNC} = a_r a_s G^*_m(a_r\omega) + \phi_{p,eff}\frac{G_N(i\omega\tau_t)^n}{(i\omega\tau_t)^n + \Gamma(n+1)}. \quad (1)$$

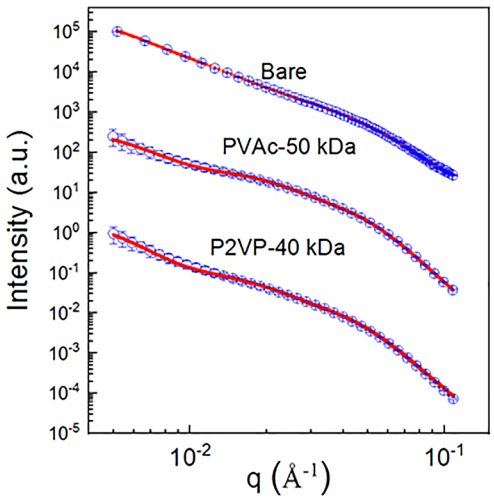

Sample	$R_{g,1}$ (nm)	p_1	$R_{g,2}$ (nm)	p_2
Bare NP	6.5	4.0	39.7	2.9
PVAc-50 kDa	7.6	4.2	37.9	2.8
P2VP-40 kDa	7.1	4.3	32.5	4.8

FIG. 1. Small-angle x-ray scattering data of poly(methyl acrylate) (PMA) nanocomposites with 30 wt. % Fe_3O_4 nanoparticle (15 nm in diameter) loading shows that dispersion in 40 kDa PMA matrix polymer is not affected by the adsorbed polymer type on particles. The two-level unified model fittings are shown with the red lines. Structural fitting parameters obtained from the two-level unified model are shown in the table. These data have been previously published in Ref. 7.

III. RESULTS AND DISCUSSION

A. Particle dispersion in PMA nanocomposites

The particle dispersion states in PMA nanocomposites were characterized by the small-angle x-ray scattering (SAXS) technique. SAXS data were analyzed using a two-level unified function,[20] which yielded 7 nm as the radius of the primary particle size and 40 nm as the average radius of the secondary structure. Fe_3O_4 particles were individually well-dispersed and secondary structures consisted of local aggregates of two particles. The SAXS data along with the unified model fits are shown in Fig. 1. Structural fitting parameters (radius of gyration of particles, R_g, and power-law exponent for the fractal dimension, $p_{1,2}$, obtained from the two-level unified model) are presented in Fig. 1. Fractal dimension, p, is determined from the slope of the SAXS profiles at a low-q regime and depends on the surface scattering and the shape of the aggregations. The first-level fractal dimension (p_1) for individual particle size analysis is $p_1 > 4$ in all samples, indicating the diffusive interphase behavior at the particle level. The second-level fractal dimension (p_2) varies in different samples. For the bare and PVAc composites, $p_2 < 3$ indicates mass fractals, and for the P2VP sample $p_2 > 4$ indicates diffusive interphases.[7] PMMA-35 kDa could not be run in SAXS; instead, particles adsorbed with other molecular weights of PMMA (10 and 188 kDa) are shown in Fig. S2 in the supplementary material. Particles were seen as aggregated fractal structures from cryotomed PMA composites in TEM. These aggregation states were not so consistent with the SAXS data collected at NSLS-II. Particles are percolated with aggregates of 100 nm or smaller as seen in TEM images (Fig. S3 in the supplementary material).

B. TTS results for entanglements

Linear viscoelastic (LVE) behavior of nanocomposites is governed by matrix and particle dynamics. Understanding the role of adsorbed polymer rigidity on matrix entanglement, relaxation, and particle diffusion is the scope of this study. We used polymers with different C_∞ values as adsorbed chains (35 kDa PMMA, $C_\infty = 7$; 50 kDa PVAc, $C_\infty = 9$; and 40 kDa P2VP, $C_\infty = 10$). Poly(methyl acrylate) (PMA 40 kDa, $C_\infty = 7$) is the matrix polymer used to disperse Fe_3O_4 nanoparticles adsorbed with different polymer rigidities. Particle loading is 30 wt. % in all samples. The adsorbed chain densities (in chains/particle) of different polymers are seen in Table I. It was shown that rigid chains (like P2VP) are more likely to be adsorbed onto particle surface[22,23] and thus form a tightly bound layer, whereas flexible chains (such as PMMA) can form loops that can entangle with other PMMA chains leading to an increased number of adsorbed chains as shown with PMMA (25 chains/particle).

The LVE data of the PMA nanocomposites are analyzed to explore the role of chain rigidity on matrix relaxation, entanglement, and particle diffusion. The intermediate time scale relaxations between the terminal relaxation (τ_t) and the entanglement relaxation time (τ_e) ($\tau_e < t < \tau_t$) is fitted by Eq. (1). The number of entanglements per chain (Z) scales as[25,26] $Z \sim \left(\frac{\tau_t}{\tau_e}\right)^{1/3}$. Figure 2 shows the LVE data of 40 kDa PMA homopolymer with $G_N = 180$ kPa, $\tau_t = 285.7$ s, $\tau_e = 0.8$ s, $M_e = 14.1$ kDa, and $Z = 7$.

TABLE I. Polymer type, molecular weight, characteristic ratio (C_∞), and number of adsorbed chains per nanoparticle used in this work.

Polymer (M.W.)	C_∞	Adsorbed chain density (chains/nanoparticle)
PMMA (35 kDa)	7	25
PVAc (50 kDa)	9	4
P2VP (40 kDa)	10	7

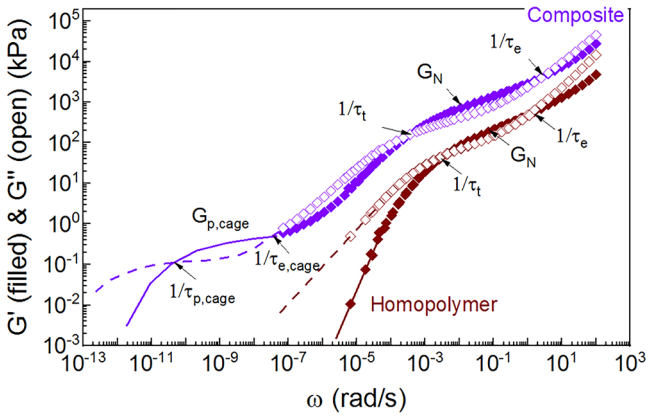

FIG. 2. Linear viscoelastic data of PMA homopolymer (40 kDa) and its composite with PMMA (35 kDa)-adsorbed Fe_3O_4 nanoparticles at 30 wt. % loading. Reference temperature is 35 °C. Low frequency response is sketched by dashed and solid lines representing the particle cage relaxations.[21] $\tau_{e,cage}$, $G_{p,cage}$, and $\tau_{p,cage}$ represent the relaxation time of particle network, the plateau modulus of particle network, and the characteristic time of diffusing particles at low frequency region, respectively.

The entanglement relaxation time (τ_e) and terminal relaxation time (τ_t) for polymer nanocomposites are shown in Fig. 2. Matrix polymer contribution to LVE data is mainly seen at short time scales ($t < \tau_e$). At intermediate time scales, nanoparticle diffusion is controlled by the local drag reduction caused by the interphase between adsorbed and matrix chains. At long times, particle dynamics dominates. As seen in Fig. 2, the terminal relaxation time (τ_t), rubber plateau modulus (G_N), and slope of storage modulus (G') of the homopolymer are very different than its composite. With the addition of nanoparticles, matrix entanglements (N_e) and particle relaxations at times $\tau_{eff} < t < \tau_{e,cage}$ are affected.[21,24,25] τ_{eff} is the effective relaxation time of polymer chains around nanoparticles and $\tau_{e,cage}$ is the relaxation time of the particle network. We will discuss this intermediate time scale relaxations in nanocomposites where dispersion is the same, but the rigidity of adsorbed polymer is different.

Adding nanoparticles is known to influence τ_t that describes the relaxation time of an entire polymer chain and N_e that is directly related to the rubber plateau modulus of the matrix polymer.[8,9,24–27] τ_t was shown to increase with particle loading in both non-attractive[9] and attractive[25] composites. It was shown that mobility and diffusion of nanoparticles can reduce entanglements of polymer matrix at time scales slower than the reptation time, leading to the speed up of matrix relaxations.[25] Recent molecular dynamics simulations on polymers filled with non-attractive nanoparticles showed that the matrix polymer disentangled and the number of entanglements per polymer chain ($Z \sim N_e^{-1}$) decreased with particle loading.[26] In another study, chain disentanglements in non-attractive poly(ethylene-propylene)–SiO_2 composite were measured in small-angle neutron scattering and neutron spin-echo experiments.[28]

The LVE data of our composites are presented in Fig. 3(a). The increase in rubber plateau of the bare PMA composite indicates that matrix entanglements enhanced with nanoparticle addition, which is consistent with the slowed terminal relaxations in an attractive composite system.[24,25] We observed that by increasing the rigidity of adsorbed chains, the rubber plateau and terminal relaxation time of the composites are decreased [Fig. 3(b)]. This is attributed to the decrease in entanglement density of the polymer. Viscosity of the composite that is normalized by its matrix homopolymer decreases with increasing rigidity of adsorbed polymers [Fig. 3(c)]. As shown, the entanglement density of the bare composite is ~40% higher than that of the homopolymer, which reveals that particle addition enhances the entanglement density in composites. Since the particle loading and dispersion state of particles are the same in all samples, the significant increase in the normalized viscosity of PMMA and PVAc samples is mainly denoted to the entanglement density enhancement as shown in the increase of rubber plateau [Figs. 3(b) and 3(d)]. In the system where P2VP is strongly adsorbed on particles but interfacial attractions between adsorbed P2VP and matrix chains are weak, Z decreases significantly [Fig. 3(d)]. The interfacial layers of flexible PMMA–PMA can entangle and diffuse easier than the highly rigid chains P2VP and PVAc. The PMA composite of the P2VP-adsorbed particle has the similar entanglement density ($Z = 7$) and normalized viscosity as in the PMA bare composite. Dynamic heterogeneity from the interfacial entanglements between PMA and adsorbed P2VP is small; thus, the plateau modulus of the composite is governed by the PMA matrix only.

High-T_g polymers adsorbed on nanoparticles may affect the mixing and entanglements at the interfacial layer of low-T_g matrix polymer. This interfacial layer can subsequently influence the diffusion behavior of nanoparticles, measured at long and intermediate time scales. Figures 4(a) and 4(b) show the model fits to the experimental viscoelastic data and the confining diffusion exponent (n) for different samples [Fig. 4(c)]. At the terminal region, PMMA-adsorbed nanoparticles have the highest G' and $n = 0.65$, suggesting a sub-diffusive motion. The particle diffusion is confined by the PMMA chains that interact and entangle with PMA in the interfacial layers, and it is unaffected by the entanglement density in the intermediate time scale. The P2VP-adsorbed nanoparticles, on the other hand, experience free diffusion ($n \sim 1$) due to their weak interphase and limited mixing between P2VP and PMA. This weak interphase can be explained with the weak drag forces mainly arising from the local viscosity around particles that contain tightly adsorbed and highly rigid P2VP chains.[2,7]

Based on the good dispersion measured in SAXS, we calculated mean-square displacement $\langle \Delta r^2 \rangle$, diffusivity (D), and viscosity (η_m) for the time range $10^3\,s < t < 10^6\,s$, which is also within the experimental time range of LVE data, as shown in Figs. S4(a)–S4(c) in the supplementary material. The calculated diffusivities vary between 10^{-1} and $10^{-4}\,nm^2/s$. Diffusion coefficient for 26 nm SiO_2 particles in 301 kDa P2VP at 180 °C was reported as $\sim 3 \times 10^{-2}\,nm^{-2}/s$.[29] Sample adsorbed with 35 kDa PMMA has the smallest $\langle \Delta r^2 \rangle$ and diffusivity (D) [Figs. S4(a) and S4(b) in the supplementary material]. The highest local viscosity is found in PMMA-adsorbed particles with the lowest rigidity as shown in Fig. S4(c) in the supplementary material. The P2VP-adsorbed particles show the opposite trend with the lowest viscosity

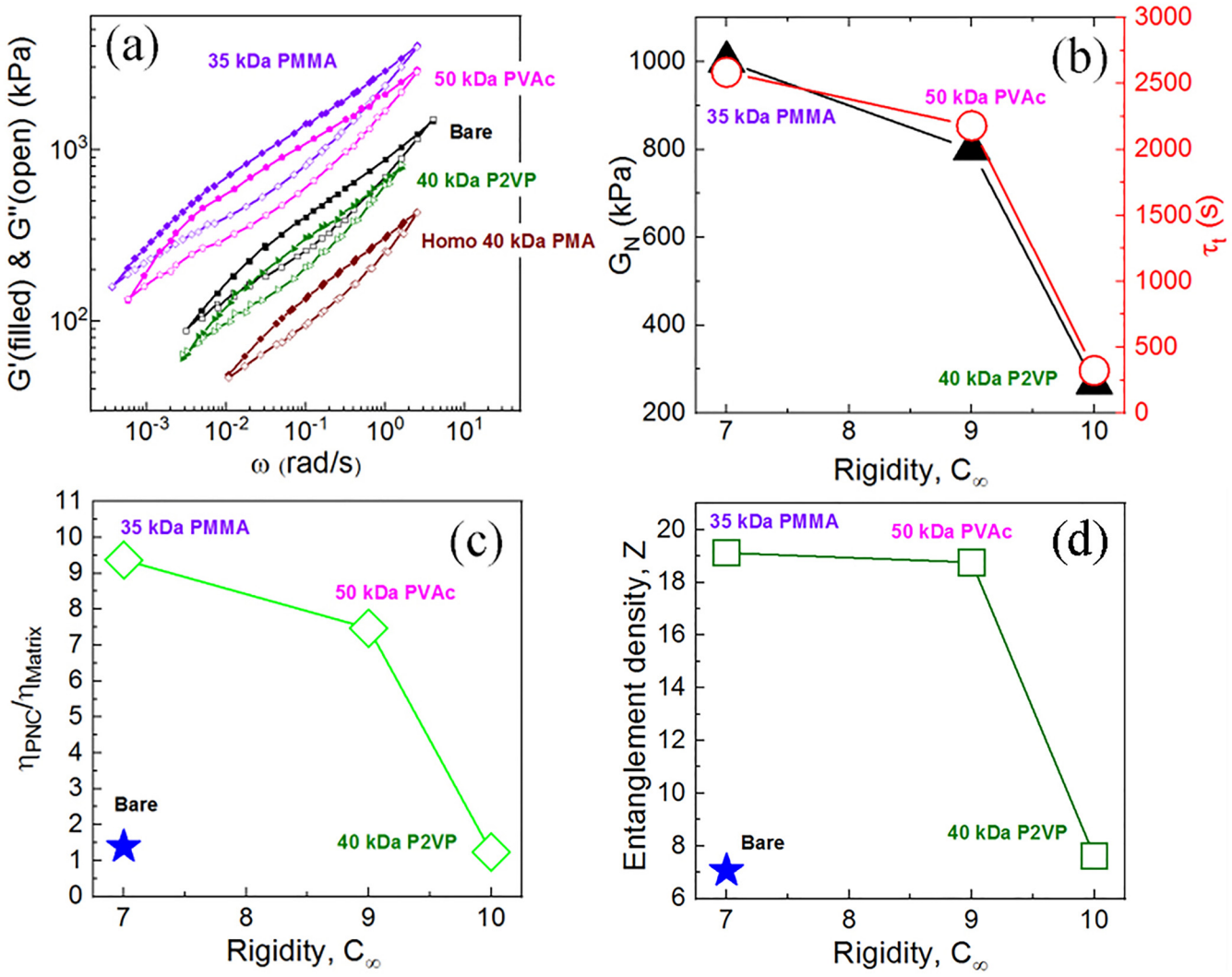

FIG. 3. (a) Linear viscoelastic data of the PMA homopolymer and PMA composites with particles adsorbed with varying rigidity of polymers (PMMA, PVAc, and P2VP). (b) Rubber plateau modulus, G_N, and terminal relaxation time, τ_t, vs rigidity of adsorbed polymer used. (c) The normalized viscosity of polymer nanocomposites of PMMA-, PVAc-, and P2VP-adsorbed Fe_3O_4 nanoparticles. (d) Number of entanglements per chain (Z) decreases with increasing rigidity of the adsorbed chain. Particle loading is 30 wt. % in all nanocomposites. Star is for the Fe_3O_4 (bare) particles in PMA.

and the largest diffusivity. The calculated time-dependent local viscosities for the sub-diffusive Fe_3O_4 nanoparticles are all lower than the dynamic viscosity of the host 40 kDa PMA homopolymer (Fig. S5 in the supplementary material). These trends are speculative since they rely on the assumption that particles are dispersed and their mobilities follow free diffusion.

Previous studies mainly focused on particle diffusion at time scales where the viscosity of the host (matrix) polymer is time independent at zero shear viscosity.[29–31] Here, we presented the time-dependent viscosity to explain the interfacial entanglements governed dynamics. We also varied the adsorbed PMMA chain length to understand the confining particle dynamics and viscosity. The preliminary data on various adsorbed chain length suggest that chain conformations and packing of adsorbed chains are critical for interfacial chain dynamics. The denser entanglements were observed with the 35 kDa PMMA compared to the 75 and 188 kDa PMMA-adsorbed chains. The fitting parameters (G_N, τ_t) for different molecular weights of adsorbed chains are presented in Fig. S6 in the supplementary material.

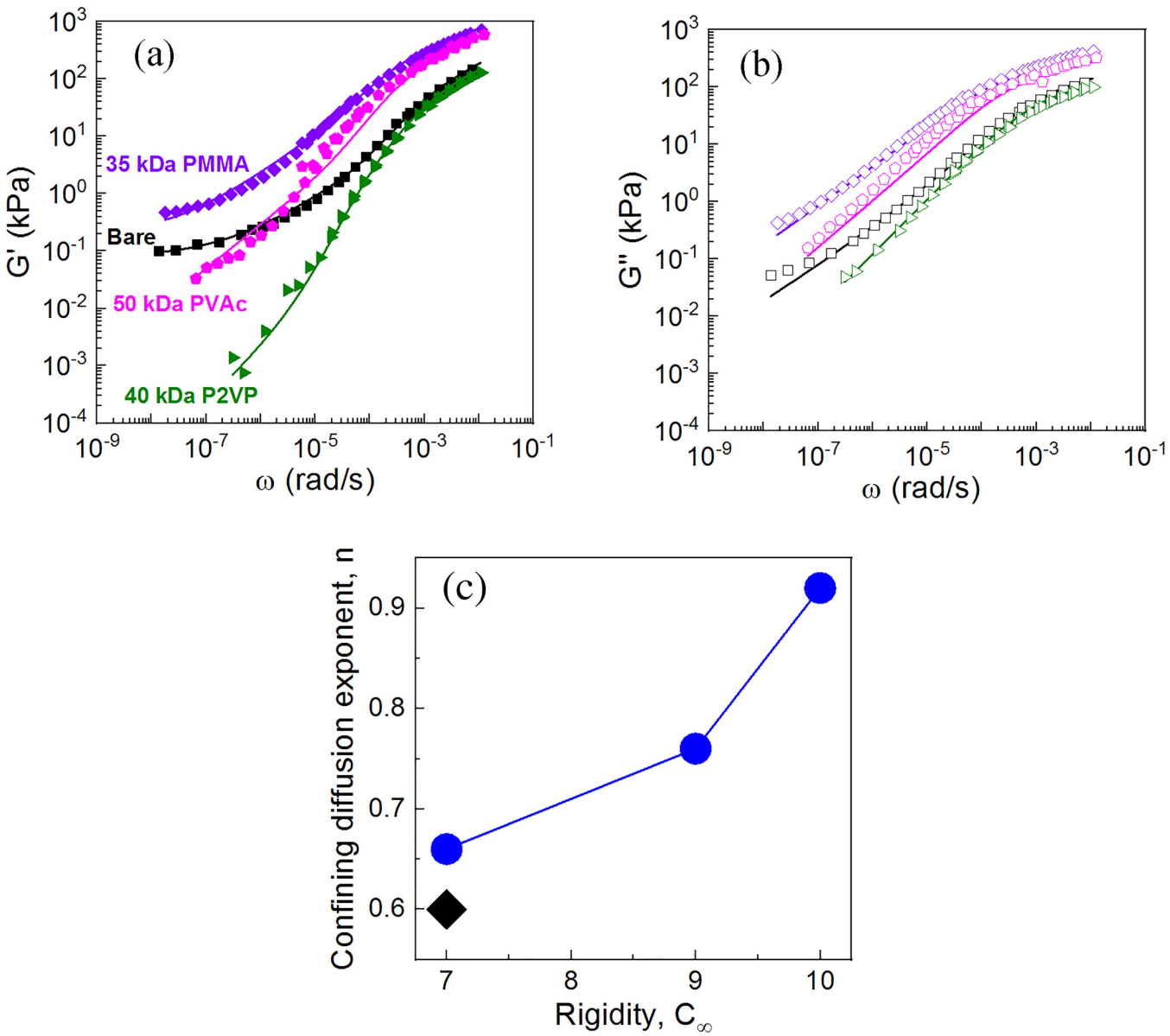

FIG. 4. (a) Storage and (b) loss moduli of PMA nanocomposites with PMMA-, PVAc-, and P2VP-adsorbed Fe_3O_4 nanoparticles within $\tau_{e,cage} < t < \tau_{e,chain}$. (c) Confining diffusion exponent (n) for particles adsorbed with different rigidity of the polymer. The black symbol is for the bare NH_2–Fe_3O_4 composite. Particle loading is 30 wt. % in all samples.

IV. CONCLUSIONS

Rigidity of adsorbed polymers influences the relaxations of matrix chains at interfacial layers in addition to the nanoparticle diffusion measured at the intermediate and long time scales. Chemical heterogeneities in interfacial layers can be used to alter the entanglement states and reptation relaxation of the matrix polymer. With flexible adsorbed PMMA chains, the rubber plateau modulus and reptation relaxation time were measured to be higher than the rigid adsorbed polymers as result of the enhanced entanglements. The confined sub-diffusion behavior of Fe_3O_4 nanoparticles with adsorbed PMMA chains indicated that particle diffusion was restricted by topological constraints of entangled chains. Furthermore, calculated diffusivity and local viscosity values showed that adsorbed chain rigidity influenced matrix relaxations and particle dynamics. Rigid adsorbed chains (P2VP) on

nanoparticles reduced the local viscosity and particles moved following Fickian diffusion, whereas particles with flexible (PMMA) chains moved in a sub-diffusive mode. Rigidity, chain length, and glass-transition temperature of polymers surrounding nanoparticles are critical factors that control the particle mobility and mechanical properties.

SUPPLEMENTARY MATERIAL

See the supplementary material for the adsorbed chain density calculation using TGA data, SAXS data analysis, TEM data of crytomed PMA nanocomposites, calculation of particle diffusivity and local viscosity, and adsorbed chain length effect on particle diffusion.

ACKNOWLEDGMENTS

This material is based on work supported by the National Science Foundation CMMI MEP Program under Grant No. 1825250.

DATA AVAILABILITY

The data that support the findings of this study are available within the article and its in the supplementary material.

REFERENCES

[1]S. Yang, S. Liu, S. Narayanan, C. Zhang, and P. Akcora, Soft Matter **14**(23), 4784 (2018).
[2]S. Yang, M. Hassan, and P. Akcora, J. Polym. Sci. Part B Polym. Phys. **57**(1), 9 (2019).
[3]E. Senses, A. Isherwood, and P. Akcora, ACS Appl. Mater. Interfaces **7**(27), 14682 (2015).
[4]C. Ding, C. Cai, L. Yin, Q. Wu, M. Pan, and C. Mei, Carbohydr. Polym. **211**, 11 (2019).
[5]T. S. Natarajan, S. Okamoto, K. W. Stöckelhuber, S. Wießner, U. Reuter, D. Fischer, A. K. Ghosh, G. Heinrich, and A. Das, ACS Appl. Mater. Interfaces **10**(18), 16148 (2018).
[6]E. Cudjoe, S. Khani, A. E. Way, M. J. A. Hore, J. Maia, and S. J. Rowan, ACS Cent. Sci. **3**(8), 886 (2017).
[7]D. Wu, D. G. Weiblen, R. Ozisik, and P. Akcora, ACS Appl. Polym. Mater. **2**(12), 5542 (2020).
[8]J. T. Kalathi, G. S. Grest, and S. K. Kumar, Phys. Rev. Lett. **109**(19), 198301 (2012).
[9]D. Kim, S. Srivastava, S. Narayanan, and L. A. Archer, Soft Matter **8**(42), 10813 (2012).
[10]E. Senses, M. Tyagi, M. Pasco, and A. Faraone, ACS Nano **12**(11), 10807 (2018).
[11]R. P. White, C. C. Price, and J. E. G. Lipson, Macromolecules **48**(12), 4132 (2015).
[12]S. Yang and P. Akcora, ACS Macro Lett. **8**(12), 1635 (2019).
[13]S. Askar, L. Li, and J. M. Torkelson, Macromolecules **50**(4), 1589 (2017).
[14]A. P. Holt, J. R. Sangoro, Y. Wang, A. L. Agapov, and A. P. Sokolov, Macromolecules **46**(10), 4168 (2013).
[15]A. P. Holt, P. J. Griffin, V. Bocharova, A. L. Agapov, A. E. Imel, M. D. Dadmun, J. R. Sangoro, and A. P. Sokolov, Macromolecules **47**(5), 1837 (2014).
[16]E. Senses, A. Faraone, and P. Akcora, Sci. Rep. **6**, 29326 (2016).
[17]A. Nimmi Das, N. Begam, M. Ibrahim, S. Chandran, V. Padmanabhan, M. Sprung, and J. K. Basu, Nanoscale **11**(17), 8546 (2019).
[18]S. Liu, E. Senses, Y. Jiao, S. Narayanan, and P. Akcora, ACS Macro Lett. **5**(5), 569 (2016).
[19]J. Ilavsky, J. Appl. Crystallogr. **45**(2), 324 (2012).
[20]G. Beaucage, J. Appl. Crystallogr. **28**(6), 717 (1995).
[21]W. You and W. Yu, Macromolecules **52**(23), 9094 (2019).
[22]E. Y. Kramarenko, R. G. Winkler, P. G. Khalatur, A. R. Khokhlov, and P. Reineker, J. Chem. Phys. **104**(12), 4806 (1996).
[23]J. M. Y. Carrillo, S. Cheng, R. Kumar, M. Goswami, A. P. Sokolov, and B. G. Sumpter, Macromolecules **48**(12), 4207 (2015).
[24]A. Karatrantos, N. Clarke, R. J. Composto, and K. I. Winey, Soft Matter **12**(9), 2567 (2016).
[25]R. Mangal, S. Srivastava, and L. A. Archer, Nat. Commun. **6**(1), 7198 (2015).
[26]Y. Li, M. Kröger, and W. K. Liu, Phys. Rev. Lett. **109**(11), 118001 (2012).
[27]M. P. Weir, D. W. Johnson, S. C. Boothroyd, R. C. Savage, R. L. Thompson, S. M. King, S. E. Rogers, K. S. Coleman, and N. Clarke, ACS Macro Lett. **5**(4), 430 (2016).
[28]G. J. Schneider, K. Nusser, L. Willner, P. Falus, and D. Richter, Macromolecules **44**(15), 5857 (2011).
[29]P. J. Griffin, V. Bocharova, L. R. Middleton, R. J. Composto, N. Clarke, K. S. Schweizer, and K. I. Winey, ACS Macro Lett. **5**(10), 1141 (2016).
[30]A. Tuteja, M. E. Mackay, S. Narayanan, S. Asokan, and M. S. Wong, Nano Lett. **7**(5), 1276 (2007).
[31]J. Park, E. J. Bailey, R. J. Composto, and K. I. Winey, Macromolecules **53**(10), 3933 (2020).